Booker, A. R., & Then, H. L. (2018). Rapid computation of L-functions attached to Maass forms. *International Journal of Number Theory*, *14*(5), 1459-1485. https://doi.org/10.1142/S1793042118500896

RAPID COMPUTATION OF L-FUNCTIONS ATTACHED TO MAASS FORMS

ANDREW R. BOOKER AND HOLGER THEN

Abstract. Let L be a degree-2 L-function associated to a Maass cusp form. We explore an algorithm that evaluates t values of L on the critical line in time $O(t^{1+\varepsilon})$. We use this algorithm to rigorously compute an abundance of consecutive zeros and investigate their distribution.

1. Introduction

In [2], the first author presented an algorithm for the rigorous computation of L-functions associated to automorphic forms. The algorithm is efficient when one desires many values of a single L-function or values of many L-functions with a common Γ-factor. In this paper, we explore the prototypical case of a family of L-functions to which that does not apply, namely Maass cusp forms in the eigenvalue aspect.

As described in [2, §5], one of the main challenges when computing L-functions is the evaluation of the inverse Mellin transform of the associated Γ-factor. Rubinstein [18] describes an algorithm based on continued fractions that performs well in practice, but for which it seems to be very difficult to obtain rigorous error bounds. On the other hand, the algorithm in [2], following Dokchitser [7], uses a precomputation based on simpler power series expansions that are easy to make rigorous; it works well for motivic L-functions of low weight, but suffers from catastrophic precision loss when the shifts in the Γ-factor grow large, as is the case for Maass forms.

A well-known similar problem occurs when one attempts to evaluate an L-function high up in the critical strip. Rubinstein, following an idea of Lagarias and Odlyzko [13], has demonstrated that this can be dealt with effectively by multiplying by an exponential factor to compensate for the decay of the Γ-factor; specifically, for a complete L-function $\Lambda(s)$ of degree d, one works with $e^{-i\theta s}\Lambda(s)$ for a suitable $\theta < \pi d/4$. This idea can be made to work for general L-functions, including those associated to Maass forms (albeit with the problems related to precision loss noted above, if the Γ-factor is not fixed), and Molin [15] has worked out rigorous numerical methods in quite wide generality.

For the specific case of Maass cusp forms, Vishe [21] (see also [9]) has shown that the "right" factor to multiply by to account for the variation in both t and the Γ-factor shifts is not the exponential function $e^{-i\theta s}$, but rather the hypergeometric function

$$ {}_2F_1\left(\frac{s+\epsilon+ir}{2}, \frac{s+\epsilon-ir}{2}; \frac{1}{2}+\epsilon; -\tan^2\theta\right) \tag{1.1}$$

where ϵ denotes the parity of the Maass form, and $\frac{1}{4}+r^2$ is its Laplacian eigenvalue. To understand the motivation for this factor, consider first the case of a classical holomorphic cuspform f, for which the L-function is defined via the Mellin transform

$$\Lambda(s) = \int_0^\infty f(iy) y^s \frac{dy}{y}.$$

Since f is holomorphic and vanishes in the cusp, we can change the contour of integration from $(0,\infty)$ to $e^{i\theta}(0,\infty)$ for some $\theta \in (-\pi/2, \pi/2)$; writing $y = e^{i\theta}u$ for $u \in \mathbb{R}$, we obtain

$$e^{-i\theta s}\Lambda(s) = \int_0^\infty f(ie^{i\theta}u) u^s \frac{du}{u}.$$

Date: September 4, 2017.

The authors wish to express their thanks to Andreas Strömbergsson and Pankaj Vishe for offering deep insight into their methods. H. T. thanks Brian Conrey, Dennis Hejhal, Jon Keating, Anton Mellit, and Franzesco Mezzadri for inspiring discussions. A. B. and H. T. acknowledge support from EPSRC grant EP/H005188/1.

Thus, Rubinstein's exponential factor arises naturally from a contour rotation.

For a Maass form f of weight 0 and even parity (say), we similarly have the integral representation

$$\Lambda(s) = \int_0^\infty f(iy) y^{s-\frac{1}{2}} \frac{dy}{y}.$$

Since f is no longer holomorphic in this case, we cannot simply rotate the contour in this expression, but we are free to start with the rotated integral $\int_0^\infty f(ie^{i\theta}u)u^{s-\frac{1}{2}}\frac{du}{u}$ and try to relate it back to $\Lambda(s)$. As we show in §2, this can be done, and the two are related essentially by the factor (1.1).

We analyze this strategy in greater detail in §2, but the upshot is that to compute Maass form L-functions for a wide range of values of r and t, it suffices to compute $f(ie^{i\theta}u)$ for suitable values of θ and u. In turn, using modularity to move each point to the fundamental domain, the problem reduces to computing the K-Bessel function $K_{ir}(y)$ for various r and y. Fortunately, that is a problem that underlies all computational aspects of Maass cusp forms and has been well studied; see, for instance, [3].

Numerical results. In §8, using as input the rigorous numerical Maass form data of [1] we compute values of the corresponding Maass form L-functions and use the resulting numerical data to test conjectures about the distribution of zeros of Maass form L-functions in the t- and r-aspects. In particular, we show that the phenomenon of zero repulsion around $\frac{1}{2} \pm ir$ that Strömbergsson observed [20] disappears in the large eigenvalue limit.

We derive rigorous error estimates and use the interval arithmetic package MPFI [17] throughout our computations to manage round-off errors. Thus, modulo bugs in the software or hardware, our numerical results are rigorous.

2. Preliminaries on Maass forms

Let $f \in L^2(\Gamma_1(N)\backslash\mathbb{H})$ be a cuspidal Maass newform and Hecke eigenform of weight 0 and level N. Then f has a Fourier expansion of the form [14]

$$f(x+iy) = \sqrt{y}\sum_{n=1}^{\infty} a_n K_{ir}(2\pi n y)\cos^{(-\epsilon)}(2\pi n x),$$

where a_n is the nth Hecke eigenvalue of f, $\frac{1}{4}+r^2$ is its eigenvalue for the hyperbolic Laplacian $-y^2\left(\frac{\partial^2}{\partial x^2}+\frac{\partial^2}{\partial y^2}\right)$, $\epsilon \in \{0,1\}$ indicates the parity, and

$$\cos^{(-\epsilon)}(x) := \begin{cases} \cos x & \text{if } \epsilon = 0, \\ \sin x & \text{if } \epsilon = 1. \end{cases}$$

Moreover, f is related to its dual $\bar{f}$ via the Fricke involution, so that

$$f(z) = w\overline{f\left(-\frac{1}{Nz}\right)}, \tag{2.1}$$

for some complex number w with $|w| = 1$.

Associated to f we have the L-function $L(s,f)$, defined for $\mathrm{Re}(s) > 1$ by the series [14]

$$L(s,f) := \sum_{n=1}^{\infty} \frac{a_n}{n^s}.$$

It follows from (2.1) that $L(s,f)$ continues to an entire function and satisfies a functional equation relating its values at s and $1-\bar{s}$. To see this, let ${}_2F_1$ denote the Gauss hypergeometric function

$${}_2F_1(\alpha,\beta;\gamma;z) := 1 + \sum_{n=1}^{\infty} \frac{(\alpha)_n(\beta)_n z^n}{(\gamma)_n n!},$$

and consider the family of Γ-factors [8]

$$\gamma_\theta(s,f) := i^{-\epsilon} w^{-1/2} \left(\frac{\cos\theta}{\sqrt{N}}\right)^{1/2-s} \Gamma_{\mathbb{R}}(s+\epsilon+ir)\Gamma_{\mathbb{R}}(s+\epsilon-ir) \cdot {}_2F_1\left(\frac{s+\epsilon+ir}{2}, \frac{s+\epsilon-ir}{2}; \frac{1}{2}+\epsilon; -\tan^2\theta\right),$$

where $\Gamma_{\mathbb{R}}(s) := \pi^{-s/2}\Gamma(s/2)$ and $\theta \in (-\pi/2, \pi/2)$ is a parameter. By [10, Sec. 6.699, Eqs. 3 and 4], we have

$$\gamma_\theta(s,f) = 4i^{-\epsilon} w^{-1/2} \left(\frac{\cos\theta}{\sqrt{N}}\right)^{1/2-s} \frac{1}{\pi^{s+\epsilon}} \int_0^\infty K_{ir}(2t) \frac{\cos^{(-\epsilon)}(2\tan(\theta)t)}{(2\tan(\theta)t)^\epsilon} t^{s+\epsilon} \frac{dt}{t} \tag{2.2}$$

for $\operatorname{Re} s > 0$. (Note that for a Maass form with odd reflection symmetry, viz. $\epsilon = 1$, (2.2) has a removable singularity at $\theta = 0$; this is related to the fact that the complete L-function is the Mellin transform of $\partial f/\partial x$ rather than f.) Making the substitution $t \mapsto \pi n \cos(\theta) u$, we can express the complete L-function $\Lambda_\theta(s,f) := \gamma_\theta(s,f)L(s,f)$ as the Mellin transform of the Maass form along a ray in the upper half plane:

$$\begin{aligned}
\Lambda_\theta(s,f) &= \gamma_\theta(s,f)L(s,f) \\
&= c_\theta(s,f) \sum_{n=1}^\infty a_n \int_0^\infty (\cos(\theta)u)^{1/2} K_{ir}(2\pi n\cos(\theta)u) \cos^{(-\epsilon)}(2\pi n \sin(\theta)u) u^{s-1/2} \frac{du}{u} \\
&= c_\theta(s,f) \int_0^\infty f(ie^{i\theta}u) u^{s-1/2} \frac{du}{u}, \qquad \text{where } c_\theta(s,f) := \frac{4w^{-1/2}}{(2\pi i \tan\theta)^\epsilon} N^{\frac{1}{2}(s-\frac{1}{2})}.
\end{aligned} \tag{2.3}$$

Splitting the integral at $u = 1/\sqrt{N}$ and employing (2.1) completes the analytic continuation:

$$\Lambda_\theta(s,f) = c_\theta(s,f) \left\{ \int_{1/\sqrt{N}}^\infty f(ie^{i\theta}u) u^{s-1/2} \frac{du}{u} + \int_0^{1/\sqrt{N}} \overline{wf\left(-\frac{1}{Nie^{i\theta}u}\right)} u^{s-1/2} \frac{du}{u} \right\}.$$

Using that $f(-\overline{z}) = (-1)^\epsilon f(z)$ and making the substitution $u \mapsto \frac{1}{Nu}$, we obtain the functional equation:

$$\begin{aligned}
\Lambda_\theta(s,f) &= c_\theta(s,f) \int_{1/\sqrt{N}}^\infty f(ie^{i\theta}u) u^{s-1/2} \frac{du}{u} + \overline{c_\theta(1-\overline{s},f)} \int_{1/\sqrt{N}}^\infty \overline{f(ie^{i\theta}u)} u^{1/2-s} \frac{du}{u} \\
&= \overline{\Lambda_\theta(1-\overline{s},f)}.
\end{aligned}$$

In particular, $\Lambda_\theta(1/2+it,f) \in \mathbb{R}$ for $t \in \mathbb{R}$.

3. Rigorous computation of L-functions

We describe an algorithm based on the fast Fourier transform that allows one to evaluate $\Lambda_\theta(s,f)$ quickly, if one is interested in many points.

The integral (2.3) is essentially a Fourier transformation,

$$\Lambda_\theta(\sigma+it,f) = c_\theta(\sigma+it,f) \int_{-\infty}^\infty f(ie^{i\theta}e^u) e^{u(\sigma-1/2)} e^{iut}\, du. \tag{2.3a}$$

Similarly for the integral (2.2),

$$\begin{aligned}
&\gamma_\theta(\sigma+it,f) \\
&\quad = c_\theta(\sigma+it,f) \int_{-\infty}^\infty (\cos(\theta)e^u)^{1/2} K_{ir}(2\pi\cos(\theta)e^u) \cos^{(-\epsilon)}(2\pi\sin(\theta)e^u) e^{u(\sigma-1/2)} e^{iut}\, du.
\end{aligned} \tag{2.2a}$$

In order to use the fast Fourier transform to compute

$$g(t) = \int_{-\infty}^\infty \hat{g}(u) e^{iut}\, du,$$

we first need to discretize the integral. To that end, let $A, B > 0$ be parameters such that $q = AB$ is an integer. In the Poisson summation formula,

$$\sum_{k\in\mathbb{Z}} g\Big(\frac{m}{A} + kB\Big) = \frac{2\pi}{B} \sum_{l\in\mathbb{Z}} e\Big(\frac{ml}{q}\Big)\, \hat{g}\Big(\frac{2\pi l}{B}\Big),$$

we solve for $g(\frac{m}{A})$, which results in

$$g\Big(\frac{m}{A}\Big) = \frac{2\pi}{B} \sum_{l=-C'}^{C} e\Big(\frac{ml}{q}\Big)\, \hat{g}\Big(\frac{2\pi l}{B}\Big) + \varepsilon_g,$$

$$\varepsilon_g := \frac{2\pi}{B} \sum_{\{l\in\mathbb{Z}: l<-C' \text{ or } l>C\}} e\Big(\frac{ml}{q}\Big)\, \hat{g}\Big(\frac{2\pi l}{B}\Big) - \sum_{k\neq 0} g\Big(\frac{m}{A} + kB\Big).$$

In §4 we will derive precise bounds for this error term.

4. Bounds

Let $Q(s, f)$ be the analytic conductor, defined by

$$Q(s, f) := N \frac{s + \epsilon + ir}{2\pi} \frac{s + \epsilon - ir}{2\pi}.$$

Note that $\gamma(s, f)$ satisfies the recurrence $\gamma(s + 2, f) = Q(s, f)\gamma(s, f)$. Further, we define

$$\chi(s, f) := \frac{\overline{\gamma(1 - \overline{s}, f)}}{\gamma(s, f)},$$

so that $L(s, f) = \chi(s, f)\overline{L(1 - \overline{s}, f)}$.

Lemma 4.1. [2, §4] *For s in the strip $\{s \in \mathbb{C} : -\frac{1}{2} \le \operatorname{Re} s \le \frac{3}{2}\}$,*

$$|L(s, f)|^2 \le |\chi(s, f)Q(s, f)| \sup_{t\in\mathbb{R}} \big|L(\tfrac{3}{2} + it, f)\big|^2.$$

Remark 4.2. The estimate in Lemma 4.1 is not optimal since, for $s = \frac{1}{2} + it$ for large t, the right-hand side grows quadratically in t, whereas the convexity estimate would give $O(t^{1+\varepsilon})$. Moreover, for $\epsilon = 0$ and $s = 1 \pm ir$ the bound becomes useless, since $|L(1 \pm ir, f)| < \infty$, whereas $\lim_{s\to 1\pm ir} |\chi(s, f)Q(s, f)| \to \infty$. Nevertheless, the estimate is clean and uniform in all parameters, and suffices for our purposes if we keep away from $s = 1 \pm ir$.

Corollary 4.3. *For s in the strip $\{s \in \mathbb{C} : \frac{1}{2} \le \operatorname{Re} s < 1\}$,*

$$|L(s, f)| \le 3N^{1/2}(|\operatorname{Im} s| + D_{s,f})$$

with

$$D_{s,f} := 3 \operatorname{Re} s - 1 + \epsilon + |r| + \frac{(2 \operatorname{Re} s - 1)^2}{1 - \operatorname{Re} s + \epsilon}.$$

Proof. Recall that $\Gamma_{\mathbb{R}}(s)$ satisfies the recurrence, reflection, and duplication formulas

$$s\Gamma_{\mathbb{R}}(s) = 2\pi\Gamma_{\mathbb{R}}(2 + s), \quad \Gamma_{\mathbb{R}}(s)\Gamma_{\mathbb{R}}(2 - s) = \frac{1}{\sin(\frac{\pi}{2}s)}, \quad \text{and} \quad \Gamma_{\mathbb{R}}(s)\Gamma_{\mathbb{R}}(1 + s) = 2^{1-s}\Gamma_{\mathbb{R}}(2s).$$

Hence, for $\epsilon \in \{0, 1\}$ and $t \in \mathbb{R}$,

$$\left|\frac{\Gamma_{\mathbb{R}}(2 + \epsilon - it)}{\Gamma_{\mathbb{R}}(1 + \epsilon + it)}\right|^2 = \left\{\begin{array}{ll} \frac{t^2 \cosh(\frac{\pi}{2}t)}{2\pi t \sinh(\frac{\pi}{2}t)} & \text{for } \epsilon = 0 \\ \frac{(1+t^2)\sinh(\frac{\pi}{2}t)}{2\pi t \cosh(\frac{\pi}{2}t)} & \text{for } \epsilon = 1 \end{array}\right\} \le \frac{(1 + \epsilon)^2 + t^2}{\pi^2},$$

which yields

$$\left|\chi(s, f)\overline{Q(1 - \overline{s}, f)}\right| \le 4N^{-1/2} |Q(s, f)|$$

for $\operatorname{Re} s = 1$.

On the critical line we have

$$\left|\chi(s,f)\frac{\overline{Q(1-\overline{s},f)}}{Q(s,f)}\right|_{\operatorname{Re} s=\frac{1}{2}}=1,$$

and by the Phragmén-Lindelöf theorem,

$$\sup_{\frac{1}{2}\le\operatorname{Re} s\le 1}\left|\chi(s,f)\frac{\overline{Q(1-\overline{s},f)}}{Q(s,f)}\right|\le\max\{4N^{-1/2},1\}\le 4.$$

Thus, in the strip $\frac{1}{2}\le\operatorname{Re} s<1$ we have

$$\left|\frac{Q(s,f)^2}{\overline{Q(1-\overline{s},f)}}\right|\le N\left(\frac{|\operatorname{Im} s|+D_{s,f}}{2\pi}\right)^2.$$

Using the Kim–Sarnak estimate [12] $p^{-\vartheta}\le|\alpha_p|\le p^{\vartheta}$ with $\vartheta=\frac{7}{64}$ in the Euler product gives

$$\sup_{\operatorname{Re} s=\frac{3}{2}}|L(s,f)|=\sup_{\operatorname{Re} s=\frac{3}{2}}\left|\prod_p\frac{1}{(1-\alpha_p p^{-s})(1-\alpha_p^{-1}p^{-s})}\right|\le\zeta(\tfrac{3}{2}+\vartheta)\zeta(\tfrac{3}{2}-\vartheta)<3\pi.$$

Inserting the last three bounds in Lemma 4.1 yields the corollary. □

Lemma 4.4. *For $s=\sigma+it$ with $0<\sigma\le 1$ and $0<\theta<\delta<\frac{\pi}{2}$,*

$$|\gamma_\theta(\sigma+it,f)|<E_{\sigma,\theta,\delta}e^{-(\delta-\theta)|t|}$$

with

$$E_{\sigma,\theta,\delta}:=\frac{|c_\theta(\sigma,f)|}{(\cos(\delta-\theta))^{1/2}}\left\{\frac{\cosh(1)\sigma^{-1}(\sigma^{-1}+\log(2)+e^{-1})}{(2\pi)^\sigma(\cos(\delta-\theta)\cos\theta)^{\sigma-1/2}}+\frac{\Gamma(\sigma-\frac{1}{2},\frac{\cos\delta}{\cos(\delta-\theta)\cos\theta})}{2(2\pi\cos\delta)^{\sigma-1/2}}\right\}.$$

Proof. For γ_θ we have the integral representation (2.2a). Since $|\gamma_\theta(\sigma-it,f)|=|\gamma_\theta(\sigma+it,f)|$, it is enough to prove the lemma for non-negative t.

Making the change of variables $u\mapsto u+i(\delta-\theta)$ and moving the contour of integration back to the real line, we get

$$g(t):=\gamma_\theta(\sigma+it,f)=\int_{\mathbb{R}}\hat{g}(u)e^{iut}\,du=\int_{\mathbb{R}}\hat{g}(u+i(\delta-\theta))e^{i(u+i(\delta-\theta))t}\,du,$$

and

$$|g(t)|\le e^{-(\delta-\theta)t}\left\{\int_{\{u\in\mathbb{R}:2\pi e^u\cos(\delta-\theta)\cos\theta<1\}}|\hat{g}(u+i(\delta-\theta))|\,du\quad+\int_{\{u\in\mathbb{R}:2\pi e^u\cos(\delta-\theta)\cos\theta\ge 1\}}|\hat{g}(u+i(\delta-\theta))|\,du\right\}.$$

We bound the first integral using the estimates $|K_{ir}(z)|\le\log\left(\frac{2}{\operatorname{Re} z}\right)+e^{-1}$ [3, p. 106] and $\left|\cos^{(-\epsilon)}(\tan(\delta-\theta)\tan(\theta)\operatorname{Im} z)\right|\le\cosh(1)$, and the second integral using $|K_{ir}(z)|<\left(\frac{\pi}{2\operatorname{Re} z}\right)^{1/2}e^{-\operatorname{Re} z}$ and $\left|\cos^{(-\epsilon)}(z)\right|\le e^{|\operatorname{Im} z|}$. □

Lemma 4.5. *For $s=\sigma+it$ with $0<\sigma\le 1$, $|t|=\frac{|m|}{A}\le\frac{B}{2}$, and $0<\theta<\delta<\frac{\pi}{2}$,*

$$\left|\sum_{k\ne 0}\gamma_\theta\Big(\sigma+i\left(\frac{m}{A}+kB\right),f\Big)\right|<\frac{E_{\sigma,\theta,\delta}}{\sinh((\delta-\theta)\frac{B}{2})}.$$

Proof. Using Lemma 4.4 together with $\left|\frac{m}{A}+kB\right|\ge(|k|-\frac{1}{2})B$ yields the stated bound. □

Lemma 4.6. *For $s=\sigma+it$ with $\frac{1}{2}\le\sigma<1$, $|t|=\frac{|m|}{A}\le\frac{B}{2}$, and $0<\theta<\delta<\frac{\pi}{2}$,*

$$\left|\sum_{k\ne 0}\Lambda_\theta\Big(\sigma+i\left(\frac{m}{A}+kB\right),f\Big)\right|<\frac{3N^{1/2}E_{\sigma,\theta,\delta}}{\sinh((\delta-\theta)\frac{B}{2})}\left(\frac{B}{2}+D_{\sigma,f}+\frac{B}{1-e^{-(\delta-\theta)B}}\right).$$

Proof. By Corollary 4.3 and Lemma 4.4,

$$|\Lambda_\theta(\sigma+it,f)| < 3N^{1/2}(|t|+D_{\sigma,f})E_{\sigma,\theta,\delta}e^{-(\delta-\theta)|t|}. \tag{4.1}$$

Applying the estimate $(|k|-\frac{1}{2})B \le \left|\frac{m}{A}+kB\right| \le (|k|+\frac{1}{2})B$ and summing up results in the stated bound. □

Lemma 4.7. *For $\frac{1}{2} \le \sigma \le 1$, $B>0$, $C \ge \frac{B}{2\pi}\log\frac{1+B/(2\pi)}{4\pi\cos\theta}$, $C' = C+\frac{B}{2\pi}\log N$, and $\hat{\Lambda}_{\sigma,\theta}(u,f) := c_\theta(\sigma,f)f(ie^{i\theta}e^u)e^{u(\sigma-1/2)}$,*

$$\left|\frac{2\pi}{B}\sum_{\{l\in\mathbb{Z}:l<-C' \text{ or } l>C\}} e\left(\frac{ml}{q}\right)\hat{\Lambda}_{\sigma,\theta}\left(\frac{2\pi l}{B},f\right)\right| < \frac{2\pi}{B}\frac{56N^{1/4}}{(2\pi\tan\theta)^\epsilon}e^{\pi\frac{C}{B}-2\pi\cos(\theta)e^{2\pi\frac{C}{B}}}.$$

Proof. Applying $|a_n| \le 2n^{1/2}$, $|K_{ir}(y)| < (\frac{\pi}{2y})^{1/2}e^{-y}$, and $\left|\cos^{(-\epsilon)}(x)\right| \le 1$ in the Fourier expansion of the Maass form gives

$$|f(x+iy)| < \frac{1}{e^{2\pi y}-1},$$

and by the Fricke involution

$$\left|f(ie^{i\theta}e^u)\right| = \left|\overline{f(ie^{-i\theta}e^{-u}/N)}\right| < \frac{1}{e^{2\pi\cos(\theta)\max\{e^u,e^{-u}/N\}}-1}. \tag{4.2}$$

For $\sigma \le 1$,

$$\left|\frac{2\pi}{B}\sum_{l>C} e\left(\frac{ml}{q}\right)\hat{\Lambda}_{\sigma,\theta}\left(\frac{2\pi l}{B},f\right)\right| < \frac{2\pi}{B}\sum_{l>C}\frac{4N^{1/4}}{(2\pi\tan\theta)^\epsilon}\frac{e^{\pi\frac{l}{B}}}{e^{2\pi\cos(\theta)e^{2\pi l/B}}-1}.$$

Writing $a := 2\pi\cos\theta$, $u := 2\pi\frac{l}{B}$, $u_0 := 2\pi\frac{C}{B}$, with $a>0$ and $u_0<u$, we have

$$\frac{e^{-ae^u+\frac{u}{2}}}{1-e^{-ae^u}} < \frac{e^{-ae^{u_0}(1+u-u_0)+\frac{u}{2}}}{1-e^{-ae^{u_0}}}.$$

Summing the resulting geometric series gives

$$\begin{aligned}\left|\frac{2\pi}{B}\sum_{l>C} e\left(\frac{ml}{q}\right)\hat{\Lambda}_{\sigma,\theta}\left(\frac{2\pi l}{B},f\right)\right| &< \frac{2\pi}{B}\frac{4N^{1/4}}{(2\pi\tan\theta)^\epsilon}\frac{e^{-ae^{u_0}+\frac{u_0}{2}}}{(1-e^{-ae^{u_0}})(1-e^{-(ae^{u_0}-\frac{1}{2})\frac{2\pi}{B}})}\\ &< \frac{2\pi}{B}\frac{4N^{1/4}}{(2\pi\tan\theta)^\epsilon}7e^{-ae^{u_0}+\frac{u_0}{2}}\end{aligned}$$

for $\frac{2\pi}{B}(ae^{u_0}-\frac{1}{2}) \ge \frac{1}{2}$, and similarly for the sum over $l<-C$.

For $\frac{1}{2} \le \sigma \le 1$,

$$\left|\frac{2\pi}{B}\sum_{l<-C'} e\left(\frac{ml}{q}\right)\hat{\Lambda}_{\sigma,\theta}\left(\frac{2\pi l}{B},f\right)\right| < \frac{2\pi}{B}\sum_{l>C'}\frac{4N^{1/4}}{(2\pi\tan\theta)^\epsilon}\frac{1}{e^{2\pi\cos(\theta)e^{2\pi l/B}/N}-1}.$$

Writing $\frac{a}{N} := \frac{2\pi\cos\theta}{N}$, $u := 2\pi\frac{|l|}{B}$, $u_0' := u_0+\log N = 2\pi\frac{C'}{B}$, with $a>0$ and $u_0'<u$, we have

$$\frac{e^{-\frac{a}{N}e^u}}{1-e^{-\frac{a}{N}e^u}} < \frac{e^{-\frac{a}{N}e^{u_0'}(1+u-u_0')}}{1-e^{-\frac{a}{N}e^{u_0'}}},$$

and summing up gives

$$\left|\frac{2\pi}{B}\sum_{l<-C'} e\left(\frac{ml}{q}\right)\hat{\Lambda}_{\sigma,\theta}\left(\frac{2\pi l}{B},f\right)\right| < \frac{2\pi}{B}\frac{4N^{1/4}}{(2\pi\tan\theta)^\epsilon}\frac{e^{-ae^{u_0}}}{(1-e^{-ae^{u_0}})(1-e^{-ae^{u_0}\frac{2\pi}{B}})}.$$

□

Lemma 4.8. *For $\frac{1}{2} \le \sigma \le 1$, $B > 0$, $C \ge \frac{B}{2\pi} \log \frac{1+B/(2\pi)}{4\pi \cos\theta}$, $C' \ge \frac{3B}{2\pi}$, and $\hat{\gamma}_{\sigma,\theta}(u,f) := c_\theta(\sigma,f)(\cos(\theta)e^u)^{1/2} K_{ir}(2\pi\cos(\theta)e^u)\cos^{(-\epsilon)}(2\pi\sin(\theta)e^u)e^{u(\sigma-1/2)}$,*

$$\left|\frac{2\pi}{B} \sum_{\{l\in\mathbb{Z}: l<-C' \text{ or } l>C\}} e\Big(\frac{ml}{q}\Big)\hat{\gamma}_{\sigma,\theta}\Big(\frac{2\pi l}{B}, f\Big)\right| < \frac{2\pi}{B}\frac{N^{1/4}}{(2\pi\tan\theta)^\epsilon}\left\{6e^{\pi\frac{C}{B}-2\pi\cos(\theta)e^{2\pi\frac{C}{B}}} + 23(\cos\theta)^{1/6}\operatorname{sech}\Big(\frac{\pi r}{2}\Big)e^{-\frac{\pi C'}{3B}}\right\}.$$

Proof. We have $|K_{ir}(y)| < (\frac{\pi}{2y})^{1/2}e^{-y}$ and $\left|\cos^{(-\epsilon)}(x)\right| \le 1$, so that

$$\left|\frac{2\pi}{B}\sum_{l>C} e\Big(\frac{ml}{q}\Big)\hat{\gamma}_{\sigma,\theta}\Big(\frac{2\pi l}{B}, f\Big)\right| < \frac{2\pi}{B}\sum_{l>C}\frac{4N^{1/4}}{(2\pi\tan\theta)^\epsilon}2^{-1}e^{-2\pi\cos(\theta)e^{2\pi\frac{l}{B}}}e^{\pi\frac{l}{B}}.$$

Writing $a := 2\pi\cos\theta$, $u := 2\pi\frac{l}{B}$, $u_0 := 2\pi\frac{C}{B}$, with $a > 0$ and $u_0 < u$, we have

$$e^{-ae^u+\frac{u}{2}} < e^{-ae^{u_0}(1+u-u_0)+\frac{u}{2}},$$

and summing the geometric series yields

$$\left|\frac{2\pi}{B}\sum_{l>C} e\Big(\frac{ml}{q}\Big)\hat{\gamma}_{\sigma,\theta}\Big(\frac{2\pi l}{B}, f\Big)\right| < \frac{2\pi}{B}\frac{4N^{1/4}}{(2\pi\tan\theta)^\epsilon}2^{-1}\frac{e^{-ae^{u_0}+\frac{u_0}{2}}}{1-e^{-(ae^u-\frac{1}{2})\frac{2\pi}{B}}} < \frac{2\pi}{B}\frac{6N^{1/4}}{(2\pi\tan\theta)^\epsilon}e^{-ae^{u_0}+\frac{u_0}{2}}$$

for $\frac{2\pi}{B}(ae^{u_0}-\frac{1}{2}) \ge \frac{1}{2}$.

The argument is slightly different for the sum over $l < -C$. Using that $\left|\cosh(\frac{\pi r}{2})K_{ir}(y)\right| < 4y^{-1/3}$ [3, p. 107] and $\left|\cos^{(-\epsilon)}(x)\right| \le 1$, we have

$$\left|\frac{2\pi}{B}\sum_{l<-C'} e\Big(\frac{ml}{q}\Big)\hat{\gamma}_{\sigma,\theta}\Big(\frac{2\pi l}{B}, f\Big)\right| < \frac{2\pi}{B}\sum_{l>C'}\frac{4N^{1/4}}{(2\pi\tan\theta)^\epsilon}\frac{4(2\pi)^{-1/3}}{\cosh(\frac{\pi r}{2})}(\cos(\theta)e^{-\frac{2\pi|l|}{B}})^{1/6} < \frac{2\pi}{B}\frac{23N^{1/4}}{(2\pi\tan\theta)^\epsilon}(\cos\theta)^{1/6}\operatorname{sech}\Big(\frac{\pi r}{2}\Big)e^{-\frac{\pi C'}{3B}}$$

for $\frac{\pi C'}{3B} \ge \frac{1}{2}$. □

Fixing the value of θ, say $\theta = \theta_1$, there is a risk of hitting a zero of γ_θ when evaluating $L(s,f) = \frac{\Lambda_\theta(s,f)}{\gamma_\theta(s,f)}$ for some specific value of t. For this reason, we will also compute for a second value of θ, $\theta = \theta_2$. The following two lemmas show that $\gamma_\theta(s,f)$ is non-zero for at least one of both values of θ.

Lemma 4.9. *For any $y \in \mathbb{R}$ with $|y| \ge 9$, $|\Gamma_{\mathbb{R}}(x+iy)|$ is an increasing function of $x \in \mathbb{R}$.*

Proof. It suffices to show that $\frac{\partial}{\partial x}\log|\Gamma_{\mathbb{R}}(x+iy)| = \operatorname{Re}\psi_{\mathbb{R}}(x+iy) > 0$. Suppose first that $x \ge 1$. Then, differentiating Binet's formula for $\log\Gamma$, we have

$$\begin{aligned}\operatorname{Re}\psi_{\mathbb{R}}(x+iy) &= \frac{1}{4}\log(x^2+y^2) - \frac{1}{2}\frac{x}{x^2+y^2} - \frac{1}{2}\log(2\pi) - \int_0^\infty\left(\frac{1}{2}-\frac{1}{2t}+\frac{1}{e^{2t}-1}\right)e^{-xt}\cos(yt)dt\\ &\ge \frac{1}{4}\log(x^2+y^2) - \frac{1}{2}\frac{x}{x^2+y^2} + \psi_{\mathbb{R}}(1) + \frac{1}{2}.\end{aligned}$$

For $x \ge 1$, this is easily seen to be minimum at $x = 1$, so we obtain

$$\operatorname{Re}\psi_{\mathbb{R}}(x+iy) \ge \frac{1}{4}\log(1+y^2) - \frac{1}{2(1+y^2)} + \psi_{\mathbb{R}}(1) + \frac{1}{2}.$$

For $x \le 1$ we use the reflection formula $\psi_{\mathbb{R}}(z) = \psi_{\mathbb{R}}(2-z) - \frac{\pi}{2}\cot(\frac{\pi}{2}z)$ to see that

$$\operatorname{Re}\psi_{\mathbb{R}}(x+iy) = \operatorname{Re}\psi_{\mathbb{R}}(2-(x+iy)) - \frac{\pi}{2}\operatorname{Re}\cot(\tfrac{\pi}{2}(x+iy)),$$

and apply the above to obtain a bound for $\operatorname{Re}\psi_{\mathbb{R}}(2-(x+iy))$. We calculate that

$$\operatorname{Re}\cot(\tfrac{\pi}{2}(x+iy)) = \frac{2e^{\pi y}\sin(\pi x)}{1-2e^{\pi y}\cos(\pi x)+e^{2\pi y}},$$

and with a little calculus we see that this is bounded in modulus by $1/\sinh(\pi\,|y|)$. Thus, altogether we have

$$\operatorname{Re}\psi_{\mathbb{R}}(x+iy) \geq \frac{1}{4}\log(1+y^2) - \frac{1}{2(1+y^2)} - \frac{\pi}{2\sinh(\pi\,|y|)} + \psi_{\mathbb{R}}(1) + \frac{1}{2}$$

for all $x \in \mathbb{R}$ and $y \neq 0$. Note that the right-hand side is strictly increasing for $y > 0$. Using the known value $\psi_{\mathbb{R}}(1) = -\frac{1}{2}(\gamma+\log(4\pi)) = -1.5541\ldots$, it is straightforward to see that $\operatorname{Re}\psi_{\mathbb{R}}(x+iy)$ is positive for $|y| \geq 9$. □

Lemma 4.10. *For $r \geq 9$, $\frac{1}{2} \leq \sigma \leq 1$, $0 < \theta_1 < \theta_2 < \frac{\pi}{2}$, $\cos\theta_1 \leq (4+\left|t^2-r^2\right|)^{-1/2}$, and $\cos\theta_2 = e^{-\frac{\pi}{2r}}\cos\theta_1$,*

$$\max\{|\gamma_{\theta_1}(s,f)|\,,|\gamma_{\theta_2}(s,f)|\} \geq \frac{2}{3}(\cos\theta_2)^{\frac{1}{2}+\epsilon}(2\pi)^{-\epsilon}\left(\frac{\pi}{r\sinh(\pi r)}\right)^{1/2}.$$

Proof. We follow the proof of [19], generalizing it and making the implied constants explicit. Using [10, Sec. 9.132, Eq. 1] and writing

$$g_\theta(s,f) := \Gamma_{\mathbb{R}}(s+\epsilon+ir)\frac{\Gamma_{\mathbb{R}}(-2ir)\Gamma_{\mathbb{R}}(1+2\epsilon)}{\Gamma_{\mathbb{R}}(1-s+\epsilon-ir)}\,{}_2F_1\left(\frac{s+\epsilon+ir}{2},\,\frac{1-s+\epsilon+ir}{2};\,ir+1;\,\cos^2\theta\right),$$

we get

$$\gamma_\theta(s,f) = i^{-\epsilon}w^{-1/2}N^{\frac{1}{2}(s-\frac{1}{2})}\left\{(\cos\theta)^{\frac{1}{2}+\epsilon+ir}g_\theta(s,f) + (\cos\theta)^{\frac{1}{2}+\epsilon-ir}\overline{g_\theta(\overline{s},f)}\right\}. \tag{4.3}$$

By Lemma 4.9, for $\sigma \geq \frac{1}{2}$ and $|t+r| \geq 9$,

$$\left|\frac{\Gamma_{\mathbb{R}}(s+\epsilon+ir)}{\Gamma_{\mathbb{R}}(1-s+\epsilon-ir)}\right| = \left|\frac{\Gamma_{\mathbb{R}}(2\sigma-1+1-\sigma+\epsilon+i(t+r))}{\Gamma_{\mathbb{R}}(1-\sigma+\epsilon-i(t+r))}\right| \geq 1.$$

Next,

$$|\Gamma_{\mathbb{R}}(-2ir)\Gamma_{\mathbb{R}}(1+2\epsilon)| = (2\pi)^{-\epsilon}\left(\frac{\pi}{r\sinh(\pi r)}\right)^{1/2},$$

and for $\frac{1}{2} \leq \sigma \leq 1$,

$$\left|\frac{(\frac{s+\epsilon+ir}{2}+n)(\frac{1-s+\epsilon+ir}{2}+n)}{(ir+1+n)(1+n)}\right| < 1 + \frac{\left|t^2-r^2\right|}{4}.$$

Hence for $\cos^2\theta \leq (4+\left|t^2-r^2\right|)^{-1}$,

$${}_2F_1\left(\frac{s+\epsilon+ir}{2},\,\frac{1-s+\epsilon+ir}{2};\,ir+1;\,\cos^2\theta\right) = 1 + \sum_{n=1}^{\infty}\Theta\left(\frac{1}{4^n}\right) = 1+\Theta\left(\frac{1/4}{1-1/4}\right),$$

where $\Theta(x)$ stands for a value of absolute size at most x.

Since $r \geq 9$, we have $|t \pm r| \geq 9$ for at least one choice of sign. Thus

$$\max\left\{|g_\theta(s,f)|\,,\left|\overline{g_\theta(\overline{s},f)}\right|\right\} \geq (2\pi)^{-\epsilon}\left(\frac{\pi}{r\sinh(\pi r)}\right)^{1/2}(1-\Theta(\tfrac{1}{3})).$$

Adjusting the phase factor $(\cos\theta)^{ir}$ in (4.3) suitably, i.e. taking $\theta = \theta_1$ and $\theta = \theta_2$ with $(\cos\theta_2)^{2ir} = e^{-i\pi}(\cos\theta_1)^{2ir}$, respectively, completes the proof. □

5. Interpolating zeros

We compute values of L on a grid, but we are ultimately interested in the zeros, which are not regularly spaced. To zoom in on the zeros, we interpolate

$$h(t) := e^{-\frac{(t-t_0)^2}{2b^2}} g(t)$$

with $g(t) = \Lambda_\theta(\sigma + it, f)$ and $g(t) = \gamma_\theta(\sigma + it, f)$, respectively. The function h has the advantage that it decays rapidly at ∞ and is approximately bandlimited, which allows us to use the Whittaker–Shannon sampling theorem [5],

$$\left| h(t) - \sum_{m\in\mathbb{Z}} h\Big(\frac{m}{A}\Big) \operatorname{sinc}\Big(\pi A\Big(t - \frac{m}{A}\Big)\Big) \right| \le 4 \int_{\pi A}^{\infty} \left|\hat{h}(u)\right| du. \tag{5.1}$$

Truncating the sum over m and bounding the error of truncation, we get an effective interpolation formula for h.

Using a sampling width of J around t_0 in the computed region $\frac{|m|}{A} \le T$, we have the following bounds.

Lemma 5.1. *For $g(t) := \Lambda_\theta(\sigma + it, f)$,*

$$\left| \sum_{\left|\frac{m}{A} - t_0\right| > J} h\Big(\frac{m}{A}\Big) \operatorname{sinc}\Big(\pi A\Big(t_0 - \frac{m}{A}\Big)\Big) \right| < \frac{6N^{1/2} E_{\sigma,\theta,\delta} \exp\big(-\frac{J^2}{2b^2}\big)}{\pi A J (1 - e^{-\frac{J}{Ab^2}})} \max\big(D_{\sigma,f}, (\delta-\theta)^{-1}\big).$$

Proof. By (4.1), we have

$$|g(t)| < 3N^{1/2} E_{\sigma,\theta,\delta} \max\big(D_{\sigma,f}, (\delta-\theta)^{-1}\big).$$

For $|m/A - t_0| = J + x$ we have

$$e^{-\frac{(\frac{m}{A} - t_0)^2}{2b^2}} \le e^{-\frac{J^2}{2b^2}} e^{-\frac{Jx}{b^2}}.$$

Together with the trivial bound $|\operatorname{sinc}(\pi A(t_0 - m/A))| \le 1/(\pi A J)$, we get

$$\begin{aligned}\left| \sum_{\left|\frac{m}{A} - t_0\right| > J} h\Big(\frac{m}{A}\Big) \operatorname{sinc}\Big(\pi A\Big(t_0 - \frac{m}{A}\Big)\Big) \right| &< \frac{3N^{1/2} E_{\sigma,\theta,\delta}}{\pi A J} \max\big(D_{\sigma,f}, (\delta-\theta)^{-1}\big) \cdot 2e^{-\frac{J^2}{2b^2}} \sum_{m=0}^{\infty} e^{-\frac{Jm}{Ab^2}} \\ &= \frac{6N^{1/2} E_{\sigma,\theta,\delta} \exp\big(-\frac{J^2}{2b^2}\big)}{\pi A J (1 - e^{-\frac{J}{Ab^2}})} \max\big(D_{\sigma,f}, (\delta-\theta)^{-1}\big).\end{aligned}$$

□

Lemma 5.2. *For $g(t) := \gamma_\theta(\sigma + it, f)$,*

$$\left| \sum_{\left|\frac{m}{A} - t_0\right| > J} h\Big(\frac{m}{A}\Big) \operatorname{sinc}\Big(\pi A\Big(t_0 - \frac{m}{A}\Big)\Big) \right| < \frac{2E_{\sigma,\theta,\delta} \exp\big(-\frac{J^2}{2b^2}\big)}{\pi A J (1 - e^{-\frac{J}{Ab^2}})}.$$

Proof. The proof is similar to that of the previous lemma, except that we bound $|g(t)|$ by Lemma 4.4 instead of (4.1). □

Lemma 5.3. *For $g(t) := \Lambda_\theta(\sigma + it, f)$, $\frac{1}{2} \le \sigma \le 1$, $u_0 \ge 0$, $\pi A \ge u_0$, and $b > 0$,*

$$\begin{aligned}4 \int_{\pi A}^{\infty} \left|\hat{h}(u)\right| du < 2 \left|c_\theta(\sigma, f)\right| \frac{e^{u_0(\sigma - \frac{1}{2})}}{1 - e^{-2\pi\cos(\theta)/\sqrt{N}}} \Bigg\{ &\frac{\sqrt{2\pi}}{2b} \operatorname{erfc}\left(\frac{b}{\sqrt{2}}(\pi A - u_0)\right) \\ &+ \frac{2e^{-u_0(\sigma-\frac{1}{2})}}{(2\pi\cos\theta)^{\sigma-\frac{1}{2}}} \Gamma\left(\sigma - \tfrac{1}{2}, 2\pi\cos(\theta) e^{u_0}\right) \Bigg\}.\end{aligned}$$

Proof. By Fourier convolution,

$$\hat{h}(v) = \frac{b}{\sqrt{2\pi}} \int_{\mathbb{R}} e^{-\frac{b^2}{2}(v-u)^2 - i(v-u)t_0} \hat{g}(u)\, du$$

with $\hat{g}(u) := c_\theta(\sigma, f) f(ie^{i\theta}e^u) e^{u(\sigma-\frac{1}{2})}$, as defined in (2.3a). Using (4.2) and writing $a := 2\pi\cos\theta$ gives

$$\left|\hat{h}(v)\right| < \frac{b}{\sqrt{2\pi}} \int_{\mathbb{R}} e^{-\frac{b^2}{2}(v-u)^2} \frac{|c_\theta(\sigma, f)|\, e^{u(\sigma-\frac{1}{2})}}{e^{a\max\{e^u, e^{-u}/N\}} - 1}\, du.$$

Changing the order of integration, we have

$$\begin{aligned} 4\int_{\pi A}^{\infty} \left|\hat{h}(v)\right| dv &< \frac{4b}{\sqrt{2\pi}} |c_\theta(\sigma, f)| \int_{\mathbb{R}} \frac{du\, e^{u(\sigma-\frac{1}{2})}}{e^{a\max\{e^u, e^{-u}/N\}} - 1} \int_{\pi A}^{\infty} dv\, e^{-\frac{b^2}{2}(v-u)^2} \\ &= 2\,|c_\theta(\sigma, f)| \int_{\mathbb{R}} \frac{e^{u(\sigma-\frac{1}{2})} \operatorname{erfc}\left(\frac{b}{\sqrt{2}}(\pi A - u)\right)}{e^{a\max\{e^u, e^{-u}/N\}} - 1}\, du. \end{aligned}$$

Let $u_0 \in [0, \pi A]$ and set $x := \frac{b}{\sqrt{2}}(\pi A - u)$. For $u < u_0$, we have $x > 0$ and $\operatorname{erfc}(x) < e^{-x^2}$, while for $u \geq u_0$, $\operatorname{erfc}(x) < 2$. Moreover, for $u < u_0$, $a > 0$, $\sigma \geq \frac{1}{2}$,

$$\frac{e^{u(\sigma-\frac{1}{2})}}{e^{a\max\{e^u, e^{-u}/N\}} - 1} < \frac{e^{u_0(\sigma-\frac{1}{2})}}{1 - e^{-a/\sqrt{N}}},$$

while for $u \geq u_0$,

$$\frac{1}{e^{a\max\{e^u, e^{-u}/N\}} - 1} < \frac{1}{(1 - e^{-a/\sqrt{N}})e^{ae^u}}.$$

Thus,

$$4\int_{\pi A}^{\infty} \left|\hat{h}(v)\right| dv < 2\,|c_\theta(\sigma, f)| \frac{e^{u_0(\sigma-\frac{1}{2})}}{1 - e^{-a/\sqrt{N}}} \left\{ \int_{-\infty}^{u_0} e^{-\frac{b^2}{2}(\pi A - u)^2}\, du + 2e^{-u_0(\sigma-\frac{1}{2})} \int_{u_0}^{\infty} \frac{e^{u(\sigma-\frac{1}{2})}}{e^{ae^u}}\, du \right\}.$$

Identifying the integrals with the complementary error function and the incomplete gamma function completes the proof. □

Lemma 5.4. *For $g(t) := \gamma_\theta(\sigma + it, f)$, $\frac{1}{2} \leq \sigma \leq 1$, $u_0 \geq 0$, $\pi A \geq u_0$, and $b > 0$,*

$$\begin{aligned} 4\int_{\pi A}^{\infty} \left|\hat{h}(u)\right| du < 2\,|c_\theta(\sigma, f)| \Bigg\{ &\frac{2}{b} e^{u_0(\sigma-\frac{1}{2})} (2\pi\cos(\theta)e^{u_0})^{1/6} \operatorname{sech}(\frac{\pi r}{2}) \operatorname{erfc}\left(\frac{b}{\sqrt{2}}(\pi A - u_0)\right) \\ &+ (2\pi\cos\theta)^{\frac{1}{2}-\sigma} \Gamma(\sigma - \tfrac{1}{2}, 2\pi\cos(\theta)e^{u_0}) \Bigg\}. \end{aligned}$$

Proof. By Fourier convolution,

$$\hat{h}(v) = \frac{b}{\sqrt{2\pi}} \int_{\mathbb{R}} e^{-\frac{b^2}{2}(v-u)^2 - i(v-u)t_0} \hat{g}(u)\, du,$$

with $\hat{g}(u) := c_\theta(\sigma, f)(\cos(\theta)e^u)^{1/2} K_{ir}(2\pi\cos(\theta)e^u) \cos^{(-\epsilon)}(2\pi\sin(\theta)e^u) e^{u(\sigma-1/2)}$, as in (2.2a). For $u < u_0$, we have $\left|\cosh(\frac{\pi r}{2}) K_{ir}(y)\right| < 4y^{-1/3}$ [3, p. 107], $\left|\cos^{(-\epsilon)}(x)\right| \leq 1$, and $e^{u(\sigma-\frac{1}{2})} < e^{u_0(\sigma-\frac{1}{2})}$. Hence, writing $\frac{a}{2\pi} := \cos\theta > 0$, we have

$$\int_{-\infty}^{u_0} e^{-\frac{b^2}{2}(v-u)^2} |\hat{g}(u)|\, du < |c_\theta(\sigma, f)|\, e^{u_0(\sigma-\frac{1}{2})} \int_{-\infty}^{u_0} e^{-\frac{b^2}{2}(v-u)^2} \frac{4(2\pi)^{-1/3}}{\cosh(\frac{\pi r}{2})} \left(\frac{a}{2\pi} e^u\right)^{1/6} du.$$

For $u \geq u_0 \geq 0$, we use $|K_{ir}(y)| < (\frac{\pi}{2y})^{1/2} e^{-y}$, and $\left|\cos^{(-\epsilon)}(x)\right| \leq 1$ to obtain

$$\int_{u_0}^{\infty} e^{-\frac{b^2}{2}(v-u)^2} |\hat{g}(u)|\, du < |c_\theta(\sigma, f)| \int_{u_0}^{\infty} e^{-\frac{b^2}{2}(v-u)^2} \frac{1}{2} e^{-ae^u} e^{u(\sigma-\frac{1}{2})}\, du.$$

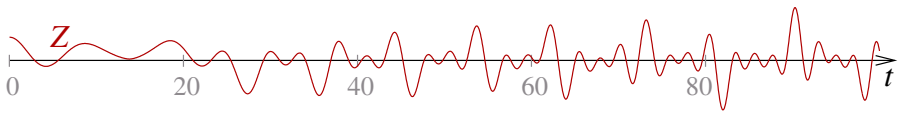

FIGURE 1. Graph of $Z(t,f)$ for the first even Maass form L-function on $\mathrm{SL}(2,\mathbb{Z})$.

Therefore, after interchanging the order of integration,

$$\begin{aligned}4\int_{\pi A}^{\infty}|h(v)|\,dv &< \frac{4b}{\sqrt{2\pi}}\,|c_\theta(\sigma,f)|\left\{e^{u_0(\sigma-\frac12)}\int_{-\infty}^{u_0}\frac{4(2\pi)^{-1/2}}{\cosh(\frac{\pi r}{2})}(ae^u)^{1/6}\int_{\pi A}^{\infty}e^{-\frac{b^2}{2}(v-u)^2}\,dv\,du\right.\\ &\qquad\left.+\int_{u_0}^{\infty}\frac12 e^{-ae^u}e^{u(\sigma-\frac12)}\int_{\pi A}^{\infty}e^{-\frac{b^2}{2}(v-u)^2}\,dv\,du\right\}\\ &< 2\,|c_\theta(\sigma,f)|\left\{e^{u_0(\sigma-\frac12)}\frac{4(2\pi)^{-1/2}}{\cosh(\frac{\pi r}{2})}(ae^{u_0})^{1/6}\int_{-\infty}^{u_0}e^{-\frac{b^2}{2}(\pi A-u)^2}\,du+\int_{u_0}^{\infty}e^{-ae^u}e^{u(\sigma-\frac12)}\,du\right\},\end{aligned}$$

where we have employed $\operatorname{erfc}(x)\le e^{-x^2}$ for $x\ge 0$, and $\operatorname{erfc}(x)<2$ otherwise. Evaluating the integrals completes the proof. □

We zoom in on the zeros using Newton's method. We estimate the derivative of h by the derivative of the sum appearing in (5.1). In principle one could derive rigorous bounds for the error along the same lines as above, but a heuristic evaluation of the derivative suffices for our purposes.

6. Detecting zeros

For each Maass form L-function under consideration, we compute rigorously many values on the critical line. For instance, Figure 1 shows a graph of

$$Z(t,f) := L(\tfrac12+it,f)e^{i\arg\gamma(\frac12+it,f)}$$

for the first even Maass form L-function on $\Gamma(1)$.

Corollary 6.1. *Let $\Omega_{\gamma_\theta} := \{t\in\mathbb{R} : \gamma_\theta(\frac12+it)=0\}$ be the set of zeros on the critical line of the Γ-factor. For values of θ_1 and θ_2 chosen according to Lemma 4.10,*

$$\Omega_{\gamma_{\theta_1}}\cap\Omega_{\gamma_{\theta_2}}=\emptyset.$$

Proof. This follows immediately from Lemma 4.10. □

Remark 6.2. Fixing the value of θ, say $\theta=\theta_1$, there is a risk of hitting a zero of γ_{θ_1} (to within the internal precision) when evaluating Z_{θ_1} for some specific value of t. In all of our computations, we never observed this in practice, i.e. we never had to deal with division by zero. However, computing at finite absolute precision, we sometimes come close to a zero of γ_{θ_1} and experience some loss of precision in the division by $|\gamma_{\theta_1}|$. Since we also compute for a second value of θ, $\theta=\theta_2$, chosen according to Lemma 4.10, we may always ensure the accuracy of the computed values of Z.

For each Maass form L-function under consideration, we rigorously compute all zeros on the critical line up to some height. The search for zeros is faciliated by the following lemma.

Lemma 6.3. *(a) Let $Z \in C^1(\mathbb{R})$ be real valued, and assume it has consecutive simple zeros at t_0, t_1 and t_2, with $Z'(t_0) > 0$. Then $\exists t_a, t_b, t_c, t_d, t_e, t_f$ such that the following holds:*

t	$Z'(t)$	$Z(t)$	*quadrant of* $Z' + iZ$
$t_a < t < t_0$	> 0	< 0	4
$t_0 < t < t_b$	> 0	> 0	1
$t_b \le t \le t_c$		> 0	1 *or* 2
$t_c < t < t_1$	< 0	> 0	2
$t_1 < t < t_d$	< 0	< 0	3
$t_d \le t \le t_e$		< 0	3 *or* 4
$t_e < t < t_2$	> 0	< 0	4
$t_2 < t < t_f$	> 0	> 0	1

(b) Let $Z \in C^n(\mathbb{R})$ be real valued, and assume it has a zero of order n at t_0, with $\left(\frac{d^n}{dt^n} Z\right)(t_0) > 0$. Then $\exists t_a, t_b$ such that the following holds:

t	$\frac{d^n}{dt^n} Z$	$\frac{d^{n-1}}{dt^{n-1}} Z$	$\frac{d^{n-2k}}{dt^{n-2k}} Z$	$\frac{d^{n-2k-1}}{dt^{n-2k-1}} Z$
$t_a < t < t_0$	> 0	< 0	> 0	< 0
$t = t_0$	> 0	$= 0$	$= 0$	$= 0$
$t_0 < t < t_b$	> 0	> 0	> 0	> 0

for $k \in \mathbb{Z}$, but $0 < 2k < n$.

Proof. The lemma follows from elementary analysis and the intermediate value theorem. □

Heuristic 6.4. *Let $Z \in C^\infty(\mathbb{R})$ be real valued. Let $(t_j)_{j \in \mathbb{N}}$ be a strictly increasing sequence of real numbers. Refine the sequence (t_j) until all zeros of Z are isolated, i.e. there is at most one zero per interval $(t_j, t_{j+1}]$.*

Remark 6.5. If the quadrants of $Z'+iZ$ for consecutive t_j are not ordered as given in Lemma 6.3(a), there is either a zero of order greater than 1 which is to be investigated according to Lemma 6.3(b), or the sequence is not yet fine enough. We expect the sequence to be fine enough if for successive t_j the quadrants of $Z' + iZ$ do change by at most by 1, and when they change, they do so in agreement with Lemma 6.3.

There is no proof that the expectation in Remark 6.5 holds, and one can construct sequences (t_j) that contradict the expectation. Nevertheless, with some reasonable choices in the construction of the sequence (t_j) and its refinements, the expectation turns out to be reliable in practice. Namely, for every Maass form L-function that we considered, we never overlooked any zero, as proven after the fact using Turing's method.

7. Turing's method

Turing's method for verifying the Riemann hypothesis for arbitrary L-functions is described in [2]. For t not the ordinate of some zero or pole of Λ, let

$$S(t) := \frac{1}{\pi} \operatorname{Im} \int_\infty^{\frac{1}{2}} \frac{L'}{L}(\sigma + it, f)\, d\sigma.$$

By convention, we make $S(t)$ upper semicontinuous, i.e. when t is the ordinate of a zero or pole, we define $S(t) = \lim_{\varepsilon \to 0^+} S(t + \varepsilon)$.

We select a particular branch of $\log \gamma(s)$ by using the principal branch of $\log \Gamma$. With this choice, set

$$\Phi(t) := \frac{1}{\pi} \operatorname{Im} \log \gamma(\frac{1}{2} + it, f). \tag{7.1}$$

We further define

$$N(t) := \Phi(t) + S(t),$$

which relates to the number of zeros in the critical strip up to height t. For $t_1 < t_2$ let Ω_L denote the multiset of zeros with imaginary part in $(t_1, t_2]$, and let $N(t_1, t_2)$ denote their number, counting multiplicity,

$$N(t_1, t_2) := \#\Omega_L(t_1, t_2).$$

Then, we have

$$N(t_1, t_2) = N(t_2) - N(t_1).$$

Theorem 7.1. [2, §4] *For $\vartheta = \frac{7}{64}$ and $\sigma > \vartheta + 1$, define*

$$z_\vartheta(\sigma) := \left(\frac{\zeta(2\sigma + 2\vartheta)\zeta(2\sigma - 2\vartheta)}{\zeta(\sigma + \vartheta)\zeta(\sigma - \vartheta)} \right)^{1/2}$$

and

$$Z_\vartheta(\sigma) := \left(\zeta(\sigma + \vartheta)\zeta(\sigma - \vartheta)\right)^{1/2}.$$

Suppose t_1 and t_2 satisfy

$$(t_i \pm r)^2 \geq \left(\tfrac{5}{2} + \epsilon\right)^2 + X^2, \quad i = 1, 2$$

for some $X > 5$, and set

$$C_\vartheta := \log Z_\vartheta\left(\frac{3}{2}\right) + \int_{3/2}^{\infty} \log \frac{Z_\vartheta(\sigma)}{z_\vartheta(\sigma)} d\sigma - \int_{3/2}^{5/2} \log z_\vartheta(\sigma) d\sigma + (\log 4) \frac{z'_\vartheta(\frac{3}{2})}{z_\vartheta(\frac{3}{2})}.$$

Then

$$\pi \int_{t_1}^{t_2} S(t)\, dt \leq \frac{1}{4} \log \left| Q\left(\frac{3}{2} + it_2\right) \right| + \left(\log 2 - \frac{1}{2}\right) \log \left| Q\left(\frac{3}{2} + it_1\right) \right| + 2C_\vartheta + \frac{2}{\sqrt{2}(X - 5)}.$$

Corollary 7.2. *For $0 \leq t_1 < t_2$, assume $\tilde{\Omega}_L(t_1, t_2)$ is a given multiset of zeros with imaginary part in $(t_1, t_2]$, i.e. $\tilde{\Omega}_L(t_1, t_2) \subseteq \Omega_L(t_1, t_2)$. Let*

$$\begin{aligned} & N_{\tilde{\Omega}_L}(t_1, t_2) := \#\tilde{\Omega}_L(t_1, t_2), \qquad \textit{counting multiplicity}, \\ & N_{\tilde{\Omega}_L}(t) := N_{\tilde{\Omega}_L}(t, 0) + \Phi(0) + S(0), \\ \textit{and} \qquad & S_{\tilde{\Omega}_L}(t) := N_{\tilde{\Omega}_L}(t) - \Phi(t). \end{aligned}$$

If

$$\pi \int_{t_1}^{t_2} \left(S_{\tilde{\Omega}_L}(t) + 1 \right) dt$$

exceeds the right-hand side of the bound in Theorem 7.1, then the set $\tilde{\Omega}_L(0, t_1)$ contains all zeros with imaginary part in $(0, t_1]$. $\tilde{\Omega}_L(0, t_1) = \Omega_L(0, t_1)$.

Proof. If $\tilde{\Omega}_L(0, t_1)$ were a proper subset of $\Omega_L(0, t_1)$, then we would have $N_{\tilde{\Omega}_L}(t_1) < N(t_1)$, whence $S_{\tilde{\Omega}_L}(t) + 1 \leq S(t)\ \forall t \in (t_1, t_2]$. But the integral of the latter is bounded by Theorem 7.1. □

8. Numerical results

We consider consecutive Maass cusp forms on $\mathrm{SL}(2, \mathbb{Z}) = \Gamma(1)$. Booker, Strömbergsson, and Venkatesh [4] have rigorously computed the first 10 Maass cusp forms on $\mathrm{SL}(2, \mathbb{Z})$ to high precision. Bian [1] has extended these computations to a larger number of Maass cusp forms. The readily available list of rigorously computed Maass cusp forms is consecutive for the first 2191 Maass cusp forms, which covers all Maass cusp forms whose Laplacian eigenvalue $\lambda = r^2 + \frac{1}{4}$ falls into the range $0 \leq r \leq 178$.

Previous numerical computations of some non-trivial zeros for a few even Maass form L-functions were made by Strömbergsson [20]. We extend his results by rigorously computing, for each of the first 2191 consecutive Maass form L-functions on $\mathrm{SL}(2, \mathbb{Z})$, many values of Z, including all non-trivial zeros up to $T = 30000$, at least.

Remark 8.1. At the time of Strömbergsson's work, even the numerical data pertaining to the Maass cusp forms for $\mathrm{SL}(2,\mathbb{Z})$ was not rigorously proven to be accurate, so he had no reason to carry out his computations of the zeros with more than heuristic estimates for the error. Making use of the rigorous data sets described above, we have rigorously verified the correctness of Strömbergsson's results. In particular his lists of zeros are consecutive and accurate. Moreover, we confirm his observation of a zero-free region on the critical line for t near r, when r is small.

We note that some theoretical results, such as Cho's theorem [6] on simple zeros of Maass form L-functions, assumed the correctness of Strömbergsson's numerical results. With our verification, Cho's theorem becomes unconditional.

Our lists of zeros contain more than 60000 consecutive non-trivial zeros per Maass form L-function. All these zeros are simple. The first several zeros of the first five Maass form L-functions are listed in Table 1.

Theorem 8.2. *For f a Maass cusp form on $\mathrm{SL}(2,\mathbb{Z})$ with spectral parameter $0 \le r \le 178$, all non-trivial zeros with $0 \le t \le 30000$ of the corresponding Maass form L-function are simple and on the critical line.*

Proof. For each Maass form L-function we prove, using Corollary 7.2, that the corresponding list of rigorously computed zeros is consecutive for $0 \le t \le 30000$, and that all the zeros are indeed simple and on the critical line. □

According to a conjecture of Montgomery [16], the distribution of non-trivial zeros should follow random matrix theory (RMT) predictions. In case of Maass form L-functions, the distribution of non-trivial zeros is expected to conform to that of eigenvalues of large random matrices from the Gaussian unitary ensemble (GUE) [11]. This raises the question of how GUE statistics relate to the zero-free region around $t = r$ observed by Strömbergsson [20]—are the GUE statistics asymptotically correct in the large t aspect only?

We investigate this question by distinguishing between zeros with small and large absolute ordinate, respectively. For a given Maass form L-function there are only a finite number of zeros with small ordinate, and the resulting statistics would be poor. Knowing the zeros for many Maass form L-functions, we can evaluate on a common scale the distribution of zeros for each L-function and collate the statistics of many of them together.

Let f be a Maass cusp form with spectral parameter r and parity ϵ. Consider the zeros of the associated Maass form L-function. We unfold the zeros,

$$x_i := \Phi(t_i)$$

with Φ from (7.1), in order to obtain rescaled zeros x_i with a unit mean density. Then $s_i := x_{i+i} - x_i$ defines the sequence of nearest-neighbor spacings, which has mean value 1 as $i \to \infty$. Now, the distribution of nearest-neighbor spacings is given by

$$\int_0^s P_f(s')\,ds' := \lim_{j\to\infty} \frac{\#\{i \le j : s_i \le s\}}{\#\{i \le j\}},$$

where the index f denotes the corresponding Maass cusp form. Distributions of rescaled nearest-neighbor spacings are expected to be independent of the specific parameter values of the corresponding Maass cusp forms f and can be collated by writing

$$P(s) := \frac{1}{\#\{f\}} \sum_f P_f(s).$$

TABLE 1. Consecutive lists of the first few non-trivial zeros for the first five Maass form L-functions on $\mathrm{SL}(2,\mathbb{Z})$. Each column is for one Maass form L-function and is specified by the spectral parameter r and the parity ϵ. The displayed numbers are the ordinates of the first few consecutive zeros for $t > 0$, all of which are on the critical line. Each number is accurate to within ± 1 in the last digit.

$r = 9.533695261$ $\epsilon = 1$	$r = 12.173008325$ $\epsilon = 1$	$r = 13.779751352$ $\epsilon = 0$	$r = 14.358509518$ $\epsilon = 1$	$r = 16.138073172$ $\epsilon = 1$
17.0249420759926	5.10553130864728	2.89772467827094	3.76470190452593	4.07043016260804
19.3441154991815	17.7442287880043	5.59124531531950	8.44187034414965	6.01471804932679
22.8261931283343	22.0828833772350	21.0903775087339	19.4483544500909	11.9094970989896
25.7999235601013	23.6900118314732	23.1575104845853	23.0939623051538	22.3497093300588
27.6164361749163	27.1426126160360	25.4393003898372	26.1518661201714	23.6756749096999
29.1018834648622	28.8988378613334	29.1892067135368	27.8260578322407	27.7899319219294
31.8310613699717	31.2199778278305	31.0617394845440	30.9903075480748	30.0381347329908
34.3471038793177	33.3027699993553	32.4527182375570	32.0681458350820	32.0229736589354
35.6095026712633	34.9413315016281	34.0272796838472	35.0463081449147	33.8112506234903
37.1600794665599	36.8220610290123	36.9312371974937	36.3730961243226	35.5014869710102
38.9798718247120	39.4036457550467	38.9870982151186	38.1758857326494	38.7878732480148
40.8649210955904	40.3954506308287	40.4655490222834	40.0803022802362	39.9476421272383
42.9624682023100	41.7518913966523	41.6851103312465	42.1472089149297	41.0312681795598
44.7165876388095	44.3141127846671	43.0510814899645	43.4072270007604	42.7546214934681
45.7081766302651	45.6041247768810	45.2203620069413	45.2854547559751	45.1517654717050
46.9228865619812	46.7731555096729	47.6607243153047	46.7361221975669	46.4771782207275
48.8845923479460	49.0623573859669	48.8179663907847	48.4727303964927	48.3625255758408
50.8585578341632	50.4428786981306	49.7984652829980	49.9790279360135	50.1639512295890
52.2084561079916	51.4839637477090	51.3751449154626	51.2742978087781	51.0355332480426
53.8667859217878	53.1358251106050	52.5598876963433	53.5712937366133	51.9925909205271
54.8124463691756	54.8229659148021	54.6535140546208	54.6096034975762	54.2915625621262
56.1642766726080	56.5390086739774	56.6899697503172	55.2759761303777	56.2796983417801
57.7477158040669	57.7030588658215	57.6166211934090	57.8055604312075	57.7013302737383
59.1886000560169	58.8511658803142	59.0433361195422	58.9190985459828	58.3383624264988
61.2112906749061	60.3363236494317	60.2512945420134	60.0205118250084	59.6802583964633
62.4099725413140	62.3427605114013	60.9302544966805	61.9578406743725	61.5356150830096
63.3997167996275	63.1451180474117	63.0554036340306	62.9609412152269	62.7868331792340
64.4782740136229	64.2165899608009	65.0280616017899	64.4328958857527	63.9997915377463
65.8411920277228	66.2554993505022	66.0531445397070	65.8735219313308	66.1489856985468
67.6680975697523	67.7507046815066	67.5747312567319	66.9654292253422	67.3268819458017
68.7657311068868	68.5590956746215	68.2882811318913	68.3575794456240	68.3016826900454
70.5658999093301	69.4453333319929	69.4223658112824	70.0897529037803	69.2840066042359
71.5151450636631	71.3077160409394	70.8802548329208	71.2206506835744	70.2797560418629
72.7793106037368	72.9519709018265	72.2899933699866	72.2540257118982	72.4309724746729
74.0609762360244	73.6890121026987	74.1574305286740	73.6822062524674	74.1819479588922
74.6049003579295	75.2952196918033	75.5105873385132	74.7169239115014	74.7011406259552
76.6307909351257	76.2065113468558	76.5116524370659	76.7494469809889	76.1335791083958
77.8404437657817	77.7272898984985	77.2965875092772	77.4226197121217	77.4636368333900
79.5177824537089	78.9591932615256	78.5268435032172	78.3595482351092	78.4634979258068
80.5991976660814	80.2505964617052	79.6462440380120	80.2707645343853	79.6781395629882
81.2939779667956	81.2013544790962	81.0934750546557	81.6367380140678	80.9175966370216
82.6785102707012	82.3915692402408	83.0999731356220	82.2630761619909	82.2205366713458
83.5676015306852	84.2017334394370	83.9810907179412	83.3558394239428	84.1953372371218
85.3322176044279	85.5004972002107	85.1204644360696	85.1612109448322	85.3999580853391
86.2362409919154	86.0646875741528	86.2039221458232	86.1020003845199	85.8048466006321
87.7201460156160	86.9821021413084	87.2818523030882	87.2123216652190	86.8146478765005
89.2073136143526	88.6357429075844	88.1416316506303	88.8839330774639	87.8727881608657
90.1509029432393	90.2062740406416	89.2944208770600	89.7818929416073	89.8827782231190
91.1018169318231	91.1589654673596	91.2299257008873	90.5922255118720	90.7761256889692
91.9180366781390	91.8841682334637	92.3569273378821	91.9914808989279	92.0942449809388
93.2577400210036	93.3261418331635	93.8884516137452	93.8202261494019	93.3990695897775
94.5361681047575	94.8381113365867	94.4624382674195	94.0923380413559	94.2940427772870
96.0183894125484	95.6998921488729	95.5004244761379	95.3961549935688	95.7412459465434
97.3452841035982	96.8603035570679	96.5910720591420	96.8178940746616	96.5775317444622
98.1159568311207	97.8041648452534	97.3209962526615	97.9968741052357	97.4404107576090
99.4221065922338	99.0948448347175	99.1562706753946	99.2448562396670	98.4151717785236
100.313745124143	100.185735184243	100.163498257903	100.278579859458	100.248850160768
101.182867524182	101.737682026863	101.758162340822	100.957059993630	101.770705877070
102.639857458614	102.777547784678	103.080823014291	102.300159307988	102.681563321248
103.546439751200	103.612872790404	103.400716986936	103.804155362774	103.496925840063
104.953553816157	104.586408006086	104.807000384562	104.874662606167	104.349526888882
106.296129428261	105.618614451690	105.510967974394	105.730976498822	105.492038316423
107.434291294864	107.487452706483	106.653239218716	106.722239502391	106.554052363134
108.433276503701	108.204341251653	107.677935083655	108.413917430577	108.328860724077
109.252032855555	109.099573594018	109.354544636483	109.104485482787	108.889566928655
109.980276788617	110.023692551348	110.858892769331	110.011383725637	109.993076784022
111.243323281265	111.610332958436	111.635310785971	111.404230185118	111.644210582933
112.822069704440	112.968244330445	112.452947413326	112.677396867124	112.766801484652
113.642166722904	113.535660411511	113.536311309751	113.308306899293	113.685480585879
114.945311219697	114.803248583420	114.599448047724	114.342832613189	114.136514740415

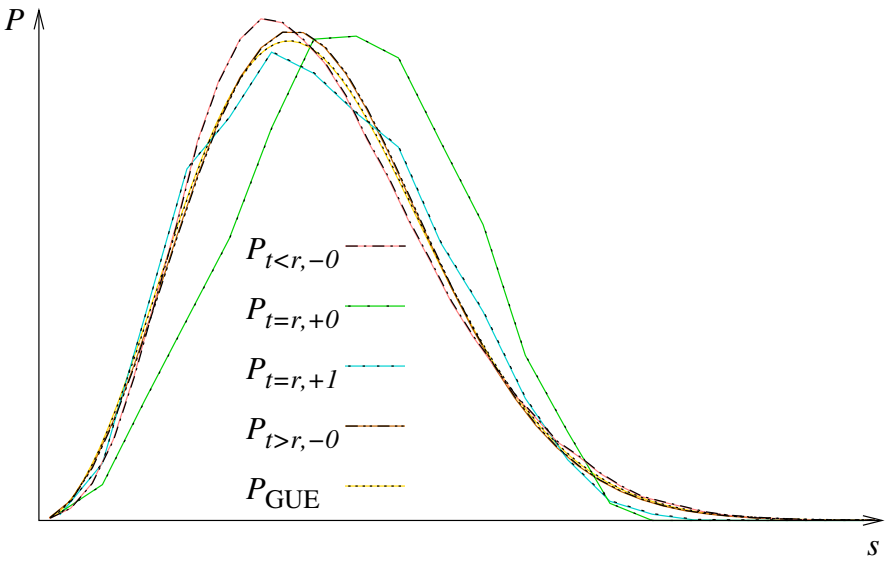

FIGURE 2. Rescaled nearest-neighbor spacing distributions $P_{t<r,-0}$, $P_{t=r,+0}$, $P_{t=r,+1}$, and $P_{t>r,-0}$, respectively, in comparison with the Wigner surmise P_{GUE}. Only the distribution of zeros that are in absolute size closest to the value of the spectral parameter might show a stronger level repulsion than the Wigner surmise. In all other cases, the distribution of zeros closely resembles GUE statistics.

To distinguish between zeros with small and large absolute ordinate, we define the respective nearest-neighbor spacings distributions,

$$\int_0^s P_{f,t<r,-n}(s')\,ds' := \lim_{j\to\infty} \frac{\#\{i\le j : s_i\le s,\ 0<t_{i-1},\ t_{i+n-1}<r\}}{\#\{i\le j : 0<t_{i-1},\ t_{i+n-1}<r\}},$$
$$\int_0^s P_{f,t=r,+n}(s')\,ds' := \lim_{j\to\infty} \frac{\#\{i\le j : s_i\le s,\ t_{i-1-n}<r<t_{i+n}\}}{\#\{i\le j : t_{i-1-n}<r<t_{i+n}\}},$$
$$\int_0^s P_{f,t>r,-n}(s')\,ds' := \lim_{j\to\infty} \frac{\#\{i\le j : s_i\le s,\ t_{i-n}>r\}}{\#\{i\le j : t_{i-n}>r\}},$$

where n is a non-negative integer, as well as their collated versions

$$P_{t<r,-n}(s) := \frac{1}{\#\{f\}}\sum_f P_{f,t<r,-n}(s),$$
$$P_{t=r,+n}(s) := \frac{1}{\#\{f\}}\sum_f P_{f,t=r,+n}(s),$$
$$P_{t>r,-n}(s) := \frac{1}{\#\{f\}}\sum_f P_{f,t>r,-n}(s).$$

For the first 2191 Maass form L-functions on $\mathrm{SL}(2,\mathbb{Z})$, the resulting distributions are displayed in Figure 2, in comparison with the Wigner surmise

$$P_{\mathrm{GUE}}(s) := \frac{32}{\pi^2}s^2 e^{-\frac{4s^2}{\pi}}.$$

As is visible, the distribution of zeros resembles GUE statistics for both small and large absolute ordinate, and there appears to be no distinction between the statistics of the two cases. Only the distribution of zeros that are in absolute size closest to the value of the spectral parameter might show a stronger level repulsion than the Wigner surmize.

However, it is unclear whether this seemingly stronger level repulsion is just an artefact of the limited number (2191) of spacings that contribute to the histogram of $P_{t=r,+0}$. If we take three

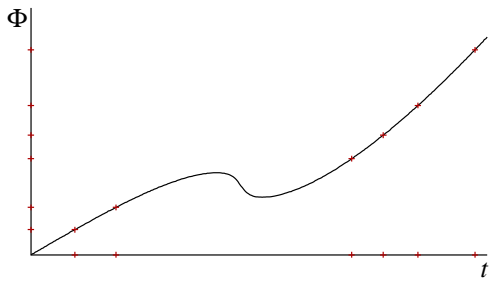

FIGURE 3. Average number Φ of non-trivial zeros for the first even Maass form L-function on $\mathrm{SL}(2,Z)$. For comparison, the locations of zeros and unfolded zeros are also included as tics. Clearly visible is the negative density region ($\Phi' < 0$) for t around r. Zeros are pulled away from this region resulting in a zero-free region in the t aspect, but not in the unfolded zeros.

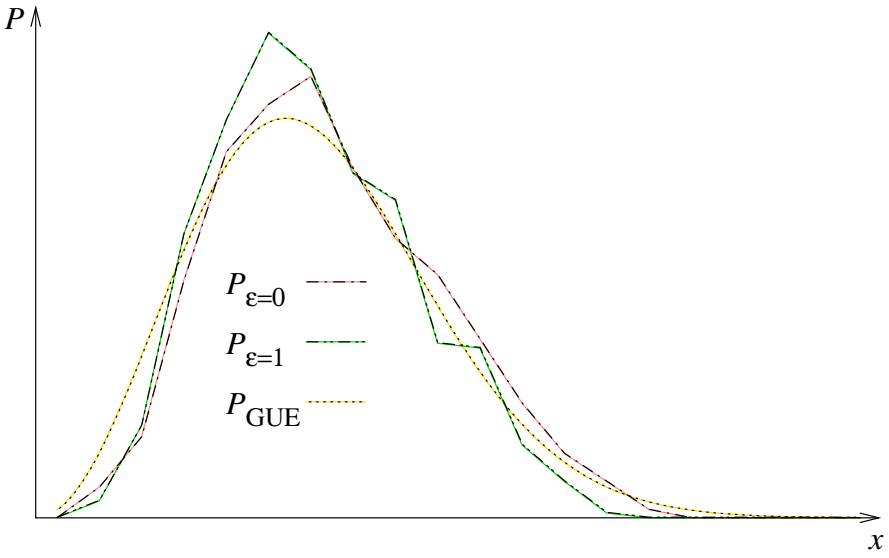

FIGURE 4. Distributions of the rescaled first zero in dependence of the parity of the Maass form L-function. Amongst the 2191 Maass cusp forms under consideration, 1018 of them are even with respect to reflection in the imaginary axis, $\epsilon = 0$, and 1173 of them are odd, $\epsilon = 1$. In comparison with the Wigner surmise P_{GUE}, close to the origin of the plots, the first zero shows a stronger level repulsion irrespective of the parity.

times as many spacings into account, as is the case with $P_{t=r,+1}$, we again find a close resemblance to the Poisson distribution. We speculate that the GUE statistics hold for all t, not only in the large t aspect.

Since the GUE statistics are based on rescaled zeros, $x_i = \Phi(t_i)$, they do not contradict a zero-free region on the critical line. The density of zeros is described by Φ', and according to the Γ-factor, the density of zeros is smaller for t in a neighborhood of r. In particular, for small values of the spectral parameter r, the density Φ' becomes negative for t near r; see Figure 3. There are finitely many Maass form L-functions on $\mathrm{SL}(2,\mathbb{Z})$ that have such a region where Φ' is negative. By inspection, we find that no zero falls into a negative density region. Moreover, the zeros seem to be repelled away from the negative density regions, resulting in the zero-free region around r.

Finally, we investigate the repulsion from zero of the rescaled first zero x_1 in dependence of the parity ϵ of the Maass form L-function. For this we consider the distributions of the rescaled first

zero,

$$\int_0^x P_{\epsilon=e}(x')\,dx' := \lim_{r\to\infty} \frac{\#\{j : x_1 < x,\ r_j \le r,\ \epsilon = e\}}{\#\{j : r_j \le r,\ \epsilon = e\}},$$

for $e \in \{0,1\}$. The resulting distributions are displayed in Figure 4. Close to the origin of the plots, they show a stronger level repulsion than the Wigner surmise $P_{\mathrm{GUE}}(x)$.

9. Parameter selection

We conclude with a more detailed description of our choices of the various parameters that occur in the algorithm. Our selection is based on heuristics and not guaranteed to be optimal, but it performs well in practice.

Let $f \in L^2(\Gamma_1(N)\backslash\mathbb{H})$ be a cuspidal Maass newform and Hecke eigenform of weight 0 and level N, parity ϵ, and spectral parameter r. We fix a choice of abscissa $\sigma \in [\frac{1}{2}, 1)$ and the maximal height $T \in \mathbb{R}_{>0}$ of the vertical line $s \in \{\sigma + it : |t| \le T\}$ on which we will compute the Maass L-function to within some desired error $\varepsilon_L > 0$.

There are a number of additional parameters in the algorithm which are implicitly given by the error analysis, such as the angle θ at which we rotate the contour of integration. In particular, we take two angles θ_1 and θ_2 in accordance with the assumptions of Lemma 4.10. The optimal choice is

$$\theta_1 = \arccos\big((4 + \max(r^2, T^2 - r^2))^{-1/2}\big),$$
$$\theta_2 = \arccos\big(e^{-\frac{\pi}{2r}}\cos\theta_1\big).$$

Further parameters are A, B, C, C', q, and δ, which enter the error bounds of §4. It would be desirable to take C and C' as small as possible while respecting all assumptions and bounds that are given in the lemmas of §4. However, the optimal choice is implicit. In order to proceed, we fix

$$\delta = \arccos\left(\frac{1}{64}\cos\theta_2\right),$$

which respects the assumptions $0 < \theta_1 < \theta_2 < \delta < \frac{\pi}{2}$.

The error bounds of Lemmas 4.5 and 4.6 each should not exceed a certain fraction of the target precision, say $\frac{1}{16}\varepsilon_L$. Hence, we solve

$$\frac{E_{\sigma,\theta,\delta}}{\sinh((\delta-\theta)\frac{B}{2})}\max\left(1,\, 3N^{1/2}\left(\frac{B}{2} + D_{\sigma,f} + \frac{B}{1-e^{-(\delta-\theta)B}}\right)\right) = \frac{1}{16}\varepsilon_L$$

in B, $B > 0$. The error bound of Lemma 4.7 should also not exceed $\frac{1}{16}\varepsilon_L$. Hence, we solve

$$\frac{2\pi}{B}\frac{56N^{1/4}}{(2\pi\tan\theta)^{\epsilon}}e^{\pi\frac{C}{B}-2\pi\cos(\theta)e^{2\pi\frac{C}{B}}} = \frac{1}{16}\varepsilon_L$$

in C, $C > 0$. By the assumptions of Lemmas 4.7 and 4.8, we must ensure that $C \ge \frac{B}{2\pi}\log\frac{1+B/(2\pi)}{4\pi\cos\theta_2}$ holds. If necessary, we increase our initial choice of C accordingly. Similarly, the error bound of Lemma 4.8 should not exceed $\frac{1}{16}\varepsilon_L$. Hence, we solve

$$\frac{2\pi}{B}\frac{N^{1/4}}{(2\pi\tan\theta)^{\epsilon}}23(\cos\theta)^{1/6}\operatorname{sech}\Big(\frac{\pi r}{2}\Big)e^{-\frac{\pi C'}{3B}} = \big(1-\frac{6}{56}\big)\frac{1}{16}\varepsilon_L$$

in C', $C' > 0$. By the assumptions of Lemma 4.8, we must ensure that $C' \ge \frac{3B}{2\pi}$ holds. If our initial choice of C' falls below $\frac{3B}{2\pi}$ then we replace C' by $\frac{3B}{2\pi}$. Typical values for B, C, and C' that we have used in our computations in §8 are on the order of 10^5, 10^5, and 10^7, respectively.

Next, we choose the value of q. In order to have enough bandwidth in the Fourier transform, q must be greater than $\max(C, C') + C$. For the FFT it is best if q is an integer power of two. The optimal choice is therefore

$$q = 2^{\lceil \log_2(\max(C,C')+1+C)\rceil}.$$

Once q has been chosen, A is determined via

$$A = \frac{q}{B}.$$

The FFT has a length of q terms, and the target precision is ε_L. Thus, the precision ε_0 to which each basic arithmetic floating point oparation is evaluated should be at least

$$\varepsilon_0 = \frac{\varepsilon_L}{q \log q}.$$

It is advisable to allow for a precision overhead of some extra digits. ε_0 is also the precision at which the Maass form f should be given numerically.

Finally, we have the parameters b, J, and u_0, which enter the error bounds of the interpolation, see §5. The optimal choice is implicit. In the proof of Lemma 5.4, we use $|K_{ir}(y)| < (\frac{\pi}{2y})^{1/2} e^{-y}$ with $y = 2\pi \cos(\theta) e^u$ and $u \geq u_0$. This estimate becomes reasonably sharp if

$$u_0 = \log\left(\frac{\frac{\pi}{2} r + \log \frac{1}{\varepsilon_0}}{2\pi \cos\theta_2} \right).$$

In Lemma 5.3, we use the same value for u_0. By the assumptions of Lemmas 5.3 and 5.4, we must ensure that $0 \leq u_0 \leq \pi A$ holds. If our initial choice of u_0 exceeds πA then we replace u_0 by πA.

The error bound of Lemma 5.3 which contains the complementary error function erfc $\big(\frac{b}{\sqrt{2}}(\pi A - u_0)\big)$ should be smaller than $\varepsilon_0 \, |\hat{g}(u)|$, where $\hat{g}(u)$ is given in the proof of the lemma. This is approximately satisfied if

$$b = \frac{\big(\frac{\pi}{2} r + \log \frac{1}{\varepsilon_0}\big)^{1/2}}{\frac{1}{\sqrt{2}}(\pi A - u_0)}.$$

We use the same value for b in Lemma 5.4.

The error bounds of Lemmas 5.1 and 5.2 each should not exceed a certain fraction of the target precision, say $\frac{1}{16}\varepsilon_L$. Hence, we solve

$$\frac{6 N^{1/2} E_{\sigma,\theta,\delta} \exp\big(-\frac{J^2}{2b^2}\big)}{\pi A J (1 - e^{-\frac{J}{Ab^2}})} \max\big(D_{\sigma,f}, (\delta - \theta)^{-1}\big) = \frac{1}{16}\varepsilon_L$$

in J, $J > 0$. Typical values for $\frac{J}{b}$ that we have used in our computations in §8 are on the order of 10^1.

We remark that the above given parameter choices are very conservative. For instance, if we take $N = 1$, $\epsilon = 1$, $r = 9.533695261\ldots$, $\sigma = \frac{1}{2}$, $T = 100$, $\varepsilon_L = 10^{-40}$, and determine all other parameters accordingly, we find after the fact that the computations are not limited to $|t| \leq 100$, but are accurate all the way up to $|t| \lesssim 2000$ with a precision of $\varepsilon_L = 10^{-40}$. Moreover, for $|t| \lesssim 5600$ the results are still accurate with a precision of $\varepsilon_L = 10^{-25}$.

References

[1] C. Bian, A. R. Booker, and M. Jacobson, Unconditional computation of the class groups of real quadratic fields, in preparation.

[2] A. R. Booker, Artin's conjecture, Turing's method, and the Riemann hypothesis, Experiment. Math. **15** (2006), 385–408.

[3] A. R. Booker, A. Strömbergsson, and H. Then, Bounds and algorithms for the K-Bessel function of imaginary order, LMS J. Comp. Math. **16** (2013), 78–108.

[4] A. R. Booker, A. Strömbergsson, and A. Venkatesh, Effective computation of Maass cusp forms, Int. Math. Res. Notices **2006** (2006), article ID 71281.

[5] J. L. Brown Jr., On the error in reconstructing a non-bandlimited function by means of the bandpass sampling theorem, J. Math. Anal. Appl. **18** (1967), 75–84.

[6] P. J. Cho, Simple zeros of Maass L-functions, Int. J. Number Theory **9** (2013), 167–178.

[7] T. Dokchitser, Computing special values of motivic L-functions, Experiment. Math. **13** (2004), 137–149.

[8] C. Epstein, J. L. Hafner, and P. Sarnak, Zeros of L-functions attached to Maass forms, Math. Z. **190** (1985), 113–128.

[9] A. Good, On various means involving the Fourier coefficients of cusp forms, Math. Z. **183** (1983), 95–129.

[10] I. S. Gradshteyn and I. M. Ryzhik, *Table of Integrals, Series, and Products*, Academic Press, 2007.

[11] J. P. Keating and N. C. Snaith, Random matrix theory and $\zeta(1/2+it)$, Commun. Math. Phys. **214** (2000), 57–89.
[12] H. H. Kim and P. Sarnak, Refined estimates towards the Ramanujan and Selberg conjectures, J. Amer. Math. Soc. **16** (2003), 139–183.
[13] J. C. Lagarias and A. M. Odlyzko, On computing Artin L-functions in the critical strip, Math. Comp. **33** (1979), 1081–1095.
[14] H. Maass, Über eine neue Art von nichtanalytischen automorphen Funktionen und die Bestimmung Dirichletscher Reihen durch Funktionalgleichungen, Math. Annalen **121** (1949), 141–183.
[15] P. Molin, Intégration numérique et calculs de fonctions L. PhD thesis, Université Bordeaux I, 2010.
[16] H. L. Montgomery, The pair correlation of zeros of the zeta function. Analytic number theory (Proc. Sympos. Pure Math. **24**, St. Louis Univ., St. Louis, Mo., 1972), pp. 181–193. Amer. Math. Soc., Providence, R.I., 1973.
[17] MPFI, multiple precision floating-point interval library, `http://perso.ens-lyon.fr/nathalie.revol/software.html`
[18] M. Rubinstein, Computational methods and experiments in analytic number theory, In *Recent Perspectives in Random Matrix Theory and Number Theory*, pp. 425–506, London Math. Soc. Lecture Note Ser. **322**, Cambridge, Cambridge Univ. Press, 2005.
[19] P. Sarnak, Fourth moments of grossencharakteren zeta functions, Comm. Pure and Appl. Math. **38** (1985), 167–178.
[20] A. Strömbergsson, On the zeros of L-functions associated to Maass waveforms, Int. Math. Res. Notices **1999** (1999), 839–851.
[21] P. Vishe, Rapid computation of L-functions for modular forms, Int. Math. Res. Notices (2012), doi:10.1093/imrn/rns112

Department of Mathematics, University of Bristol, University Walk, Bristol, BS8 1TW, United Kingdom, e-mail: andrew.booker@bristol.ac.uk

Alemannenweg 1, 89537 Giengen, Germany, e-mail: holger.then@bristol.ac.uk